Barbara LISIECKA*, Agata DUDEK*

MODIFICATION OF THE SURFACE LAYER OF SINTERED DUPLEX STAINLESS STEELS THROUGH ALLOYING USING THE GTAW METHOD

MODYFIKACJA WARSTWY WIERZCHNIEJ SPIEKANYCH STALI NIERDZEWNYCH POPRZEZ STOPOWANIE METODĄ GTAW

Key words: wear resistance, coefficient of friction (COF), Cr3C2 coating, surface layer alloying, sintered duplex stainless steel (SDSS), powder metallurgy (PM), gas tungsten arc welding (GTAW).

Abstract The demand for materials obtained using powder metallurgy (PM) is constantly increasing, especially on SDSSs, which are characterized by a two–phase structure consisting of ferrite and austenite. The main purpose of this study was to examine the effect of surface layer alloying with chromium carbide on the microstructure and tribological properties (e.g., hardness and wear resistance) of SDSSs. The multiphase sinters were prepared from two types of water–atomized steel powders: 316L and 409L. The technique of the APS method was used to deposit Cr_3C_2–NiAl powder on the SDSS surface. Electric arc (GTAW method) was used for surface alloying. Optical and scanning microscopy, X–ray phase analysis, and examinations of microhardness and coefficient of friction were performed in order to determine the microstructure and basic properties of SDSS after alloying. The surface alloying with Cr_3C_2 improves tribological properties of SDSSs such as hardness and the coefficient of friction.

Słowa kluczowe: odporność na ścieranie, współczynnik tarcia, powłoka Cr3C2, stopowanie warstwy wierzchniej, spiekana stal nierdzewna typu duplex (SDSS), metalurgia proszków (PM), spawanie łukowe (GTAW).

Streszczenie Zapotrzebowanie na materiały otrzymywane przy użyciu metalurgii proszków stale rośnie, szczególnie na spiekane stale duplex, które charakteryzują się dwufazową strukturą składającą się z ferrytu i austenitu. Głównym celem pracy było zbadanie wpływu stopowania warstwy wierzchniej z węglikiem chromu na mikrostrukturę i własności tribologiczne (np. twardość, odporność na zużycie) spiekanych stali. Wielofazowe spieki przygotowano z rozpylanych wodą komercyjnych proszków stalowych 316L i 409L. W celu wytworzenia powłoki z proszku Cr_3C_2–NiAl na powierzchni SDSS zastosowano metodę APS. Obróbkę przetopieniową spieków przeprowadzono spawalniczą metodą łukową GTAW. W celu analizy mikrostruktury i podstawowych własności spieków po stopowaniu przeprowadzono analizę z wykorzystaniem mikroskopii optycznej, skaningowej, fazową analizę rentgenowską oraz badania twardości i określenie współczynnika tarcia. Stopowanie powierzchni z Cr_3C_2 poprawia własności tribologiczne spieków, takie jak twardość i współczynnik tarcia.

INTRODUCTION

Technology used for the manufacturing of structural materials from metallic powders with an addition or without an addition of non–metallic powders as a result of processes of forming and sintering is called powder metallurgy (PM) [**L. 1**]. An extremely important and dynamically growing sector of the PM industry is the production of stainless steel components. Sintered duplex stainless steels (SDSSs) are an interesting class of engineering materials, and they are widely used in many sectors, mainly in highly industrialized countries. The sintered products are using in several technological applications in the food processing, chemical, aerospace, automotive, and medical industries. Currently, the largest consumer of SDSS products is the automotive industry (ca. 73% of all sinters). These products are mainly used to manufacture automotive parts, such as exhaust

* Czestochowa University of Technology, Institute of Material Engineering, Faculty of Production Engineering and Materials Technology, Czestochowa, Poland, e-mail: lisiecka.barbara@wip.pcz.pl, e-mail: dudek.agata@wip.pcz.pl.

system components (flanges and sensors), antilock brake systems (ABS) sensors rings, turbocompressors, bearings, gears, filters, pumps, and other systems [**L. 2, 3**].

The PM method allows one to modify the chemical composition, which makes it possible to receive a sintered duplex structure with different proportions of the two basic structural components (austenite and ferrite). An important factor affecting the microstructure of sintered duplex stainless steels is sintering time. In addition, the mechanical and functional properties depend on the chemical composition, the contribution of individual powders, the distribution of the main alloying elements (Cr/Ni) between these phases, and sintering conditions [**L. 4, 5**]. SDSSs analyzed are distinguished by high mechanical strengths, wear resistance, high toughness, and good corrosion resistance. The main disadvantage of SDSSs, which can reduce their mechanical properties under static and dynamic loading, is porosity. Additionally, the porosity features produce negative effects on the corrosion and oxidation behaviour of SDSSs, because the pores are potential sites for corrosion product accumulation. In order to improve the discussed properties, it is necessary to apply surface modification by the formation of appropriate coatings [**L. 6–9**].

Modification of surface properties of engineering materials, especially sintered duplex stainless steels, can be carried out during the coating process or surface treatments. An interesting surface modification processes is the formation of a coating based on chromium carbide, where the most well–known chromium carbide is Cr_3C_2, which has the best mechanical properties and appropriate adhesion to substrate. The chromium carbide coatings presents unique corrosion resistance and they are characterized by good the tribological properties such as more high hardness, wear resistance and strength than other carbides at high temperature [**L. 10–12**]. To produce such a coating, the atmospheric plasma spraying (APS) method is used, which enjoys unflagging interest. The APS method is a versatile thermal spray process, which can be used to deposit powders as dense, adherent, and homogeneous coatings with low porosity. During plasma spraying, the coating material in the form of powder (e.g., Cr_3C_2) is heated to a molten state. The heated material is propelled in a plasma jet towards a substrate, where the formed a deposits adhere to the substrate as coatings. Plasma spray coatings can be easily controlled to produce the desired properties of thickness, porosity, roughness, and hardness [**L. 13–15**].

Gas tungsten arc (GTA) or tungsten inert gas (TIG) welding processes are the most common fabrication processes employed for modification of a surface layer of SDSSs which show porosity. In the GTAW, the heat required for welding is generated by a cone-shaped electric arc, which is established between the non–consumable tungsten electrode and the melted metal. The molten metal is shielded from atmospheric contamination by an inert gas (e.g., argon). A valuable advantage encouraging the use of this method is the ability to modify the surface in terms of hardness and the coefficient of friction [**L. 16–19**].

MATERIAL AND METHODS

The specimens for the investigations were obtained from water–atomized powders of 316 L steel and ferritic 409 L steel manufactured by Höganäs (Sweden). The chemical composition of steel powders is presented in **Table 1**. Both powders selected had a nominal particle size of 150 μm.

Table 1. Chemical composition of steel powders (%wt.)
Tabela 1. Skład chemiczny proszków stalowych (% mas.)

Powder grade	Cr	Ni	Mo	Si	Mn	C	S	Fe
316 L	16.80	12.00	2.00	0.90	0.10	0.022	0.005	Balance
409 L	11.86	0.14	0.02	0.82	0.14	0.020	0.010	Balance

The powders were mixed at different proportions of ferritic and austenitic steel powders to obtain the different series of the samples (see **Table 2**). The powders were uniaxially compacted with the addition of 1% Acrawax C lubricant at 650 MPa. The molded pieces were sintered at the temperature of 1250°C for 40 minutes and then cooled down with a cooling rate of 0.5°C/s. In order to significantly limit the oxidation of the batch and protect from reduction of the chromium content, the whole process was carried out in a reducing atmosphere using hydrogen.

Table 2. Percentage contribution of individual powders [%]
Tabela 2. Procentowy udział poszczególnych proszków [%]

Powder grade	Series number		
	1	2	3
316 L	100%	50%	0%
409 L	0%	50%	100%

To improve functional properties of SDSSs, a modified layer from chromium carbide was formed. Due to the fact that the coating is made at high temperatures, chromium carbide is mixed with nickel and aluminium. The whole process was carried out

using atmospheric plasma spraying (APS method) with the application of the Cr_3C_2 + 10% NiAl. The resulting coating had a thickness of around 60 μm.

The next step was alloying the coatings (using GTAW technology) at an optimal current intensity of 60A and voltage parameters. The alloying treatment was carried out with constant surface scanning (340 mm/min) and the shielding gas was argon, with the flow set at ~ 14 l/min.

The analysis of the microstructure after the application of Cr_3C_2–NiAl powder and surface alloying was carried out using an optical microscope Olympus GX41 and a scanning microscope Jeol JSM–6610LV. The macroscopic evaluation of SDSSs after the alloying process was performed using a stereo microscope Olympus SZ61. The Vickers methodology (with the load of 980.7 mN) was employed to measure the microhardness of SDSSs obtained by the Shimadzu HMV–G Series.

The identification of phase composition was made using an X–ray diffractometer (Seifert 3003 T–T) with a cobalt lamp with a characteristic radiation wavelength of $\lambda_{cok\alpha}$ = 0.17902 nm. Other parameters were the following: supply voltage: Ur = 30–40 kV, current intensity Ir = 30–40 mA, angle range: 2θ = 10–120°, measurement step: 0.1°, and pulse integration time tr = 10 s.

The scratch resistance test (Revetest XPress Plus using Rockwell indented tip) was performed in order to determine the coefficient of friction for SDSSs obtained in the investigation. The following parameters were maintained during the test: permanent load of 10 N, scratch length 10 mm, and scratch rate 5 mm/min.

RESULTS AND DISSCUSION

The grains of Cr_3C_2–NiAl powder and maps of the distribution of elements of the analysed powder obtained by the scanning microscope Jeol JSM–6610LV are presented in **Figure 1**.

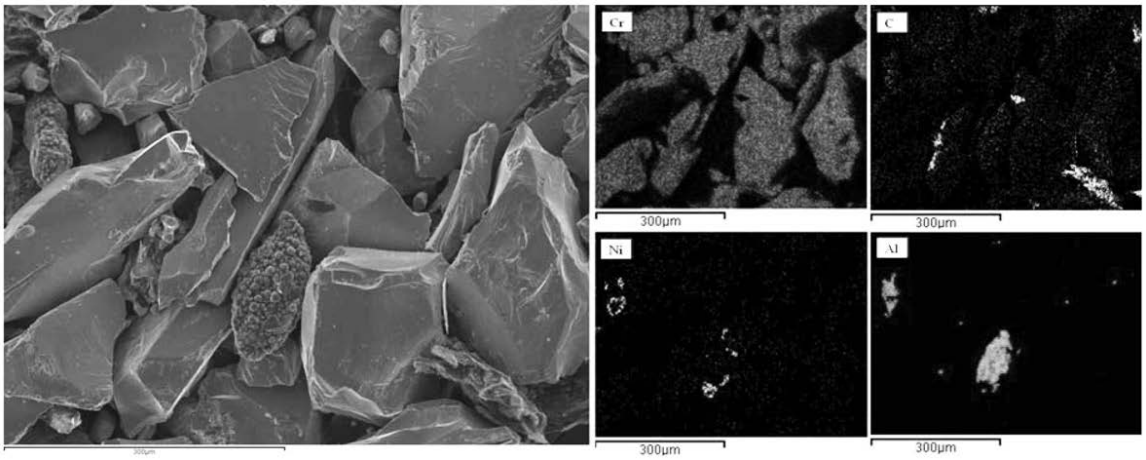

Fig. 1. Morphology and maps of the distribution of elements of the Cr_3C_2–NiAl powder used to produce the coating
Rys. 1. Morfologia i mapy rozkładu pierwiastków proszku Cr_3C_2–NiAl użytego do wytworzenia powłoki

The chromium carbide coating deposited using the APS method on the SDSSs had a thickness of around 60 μm. **Figure 2** presents the cross–section of the coating's microstructure obtained from the scanning microscope Jeol JSM–6610LV.

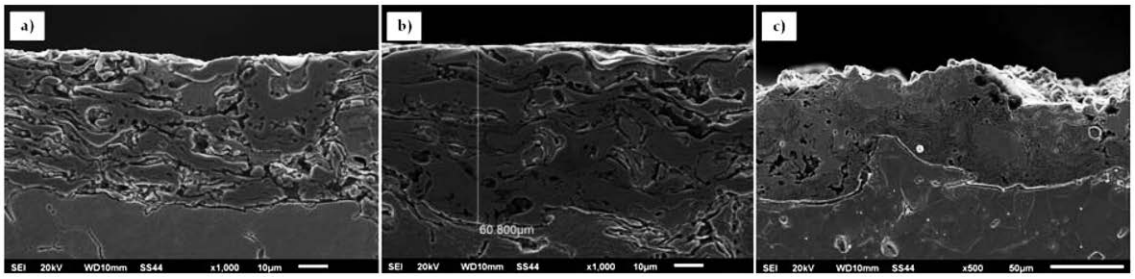

Fig. 2. Microstructure of the coating after APS process for SDSSs: a) 100% 316L, b) 50% 316L + 50% 409L, c) 100% 409L
Rys. 2. Mikrostruktura powłoki po procesie APS dla spieków: a) 100% 316L, b) 50% 316L + 50% 409L, c) 100% 409L

The alloying on the surface was used for macroscopic examinations, with the main criteria including band continuity, comparable width, and a relatively smooth surface without defects (i.e. craters, cracks). These requirements were met for the bands alloyed using the GTAW method at a current intensity 60 A. **Figure 3** illustrates the morphology of the surface after the alloying process for SDSSs obtained by stereo microscope Olympus SZ61.

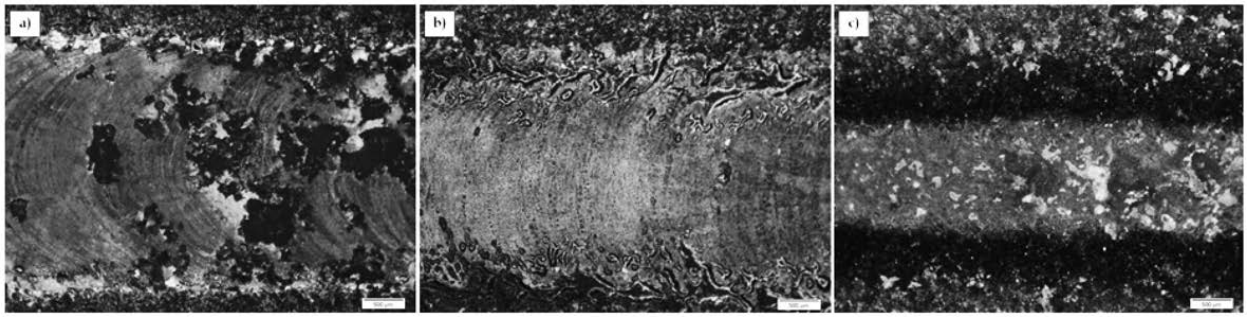

Fig. 3. Topography of the surface of SDSSs after alloying 60 A: a) 100% 316L; b) 50% 316L + 50% 409L; c) 100% 409L

Rys. 3. Topografia powierzchni spieków po stopowaniu 60 A: a) 100% 316L, b) 50% 316L + 50% 409L, c) 100% 409L

The microstructures were observed using the metallographic sections etched with aqua regia. **Figure 4** presents the microstructure obtained for 100% 316L steel after surface alloying treatment at 60 A by the optical microscope Olympus GX41.

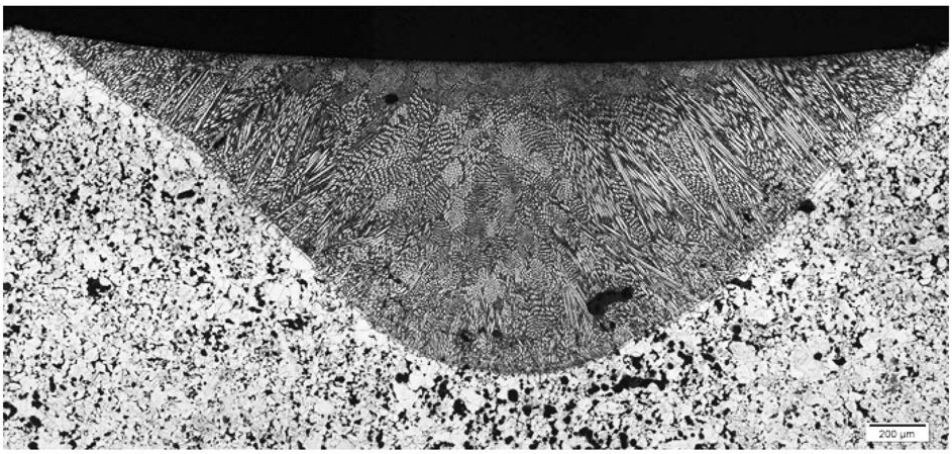

Fig. 4. Microstructure of the entire alloyed zone for 100% 316L steel

Rys. 4. Mikrostruktura strefy stopowanej dla stali 100% 316L

Microstructure analysis of the surface layers revealed a homogeneous cellular–dendritic structure after alloying treatment. The presence of columnar crystals oriented according to the direction of heat transfer was caused by the fast heat transfer and high gradient of temperature. The transient zone, obtained by the contact of the alloyed layer with base material, was the location of the nucleation and growth of primary structure crystals.

Figure 5 presents the microstructure of the surface after the alloying process obtained for 100% 409L steel by the scanning microscope Jeol JSM–6610LV.

Table 3 presents an analysis of chemical composition of the surface layers in SDSSs after alloying using the GTAW method. The analysis was aimed at a comparison areas obtained for SDSSs after surface treatment, the determination of the migration process of alloying elements (Cr, Ni) during crystallization process, and the determination of the degree of the homogeneity of the chemical composition in surface layers.

Examination of the surface layer's alloying revealed the migration of Cr and Ni during sintering caused by the diffusion process. The content of Cr and Ni outside the boundary of the alloying zone and heat affected zone

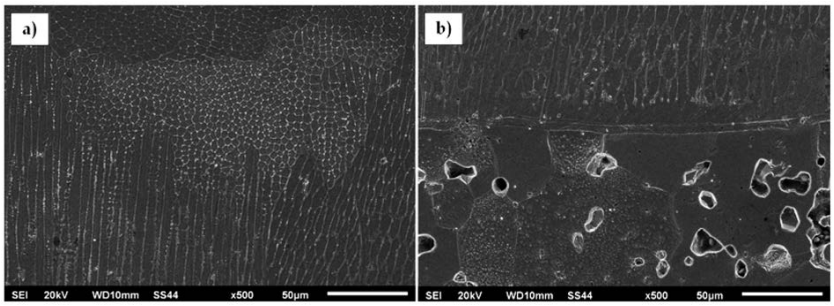

Fig. 5. Microstructure of the surface of 100% 409L steel after alloying 60 A: a) upper part of the alloyed zone, b) boundary of the alloying zone and heat affected zone

Rys. 5. Mikrostruktura powierzchni dla stali 100% 409L po stopowaniu 60 A: a) górna część strefy stopowanej, b) granica strefy stopowanej i strefy wpływu ciepła

Table 3. EDX–analysis of chemical composition of the SDSSs after alloying

Tabela 3. Analiza składu chemicznego stali spiekanych duplex po stopowaniu

SDSSs	Element	Weight [%]		
		Alloying zone	Heat affected zone	Native material
100% 316L	Cr	17.15	16.61	16.87
	Fe	63.20	62.98	63.06
	Ni	13.80	12.94	12.87
50% 316L + 50% 409L	Cr	14.21	14.46	13.45
	Fe	68.52	64.47	70.38
	Ni	15.29	14.88	5.66
100% 409L	Cr	10.77	10.69	10.68
	Fe	70.61	70.85	83.44
	Ni	15.75	15.33	4.17

decreases linearly, while the content of Fe increased. The diffusion of chromium to ferrite and nickel to austenite causes the appearance of phase transformations.

Figure 6 presents the identification of the phase composition of the 50% 316L + 50% 409L steel obtained based on X–ray phase analysis. The results of the analysis of the chromium carbide coating, the surface after alloying, and native material are showed in **Figure 6**.

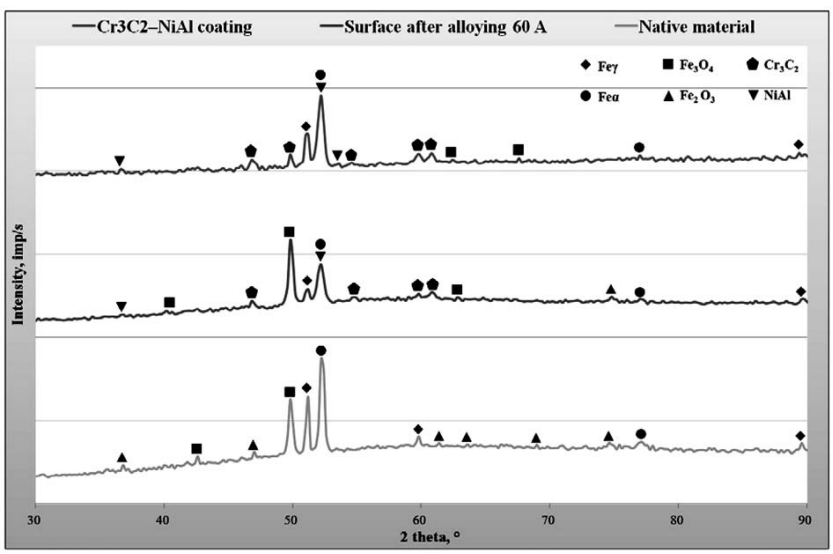

Fig. 6. Diffractograms of the 50% 316L + 50% 409L steel

Rys. 6. Dyfraktogramy spieku 50% 316L + 50% 409L

The phase composition analysis for 50% 316L + 50% 409L steel showed the presence of the following phases:

- The ferritic phase crystallizes in cubic cells with parameters a = b = c = 0.286 nm, α = β = γ = 90°.
- The austenitic phase crystallizes in cubic cells with parameters a = b = c = 0.359 nm, α = β = γ = 90°.
- The iron oxide Fe_3O_4 phase crystallizes in cubic cells with parameters a = b = c = 0.840 nm, α = β = γ = 90°.
- The iron oxide Fe_2O_3 phase crystallizes in cubic cells with parameters a = b = c = 0.835 nm, α = β = γ = 90°.
- The Cr_3C_2 phase crystallizes in the orthorhombic cells with parameters a = 0.55 nm, b = 1.14 nm, c = 0.28 nm, α = β = γ = 90°.
- The NiAl phase crystallizes in the cubic cell of Pm3m with parameters a = b = c = 0.28 nm, α = β = γ = 90°.

The peak intensities on the diffractogram obtained for SDSSs depends on the amount of individual phases in sintered steels.

Hardness measurements by the Vickers method were done to evaluate mechanical properties. **Table 4** presents the hardness of the chromium carbide coating, alloying zone, heat affected zone, and native material received during and after alloying at a current intensity of 60 A. The results represent the mean of five measurements.

Table 4. Hardness of SDSSs
Tabela 4. Twardość spiekanych stali duplex

SDSSs		Hardness [HV 0.1]		
	Cr_3C_2–NiAl coating	Alloying zone	Heat affected zone	Native material
100% 316L	246 ±19	164 ±4	150 ±6	111 ±17
50% 316L + 50% 409L	266 ±17	153 ±13	148 ±10	113 ±19
100% 409L	285 ±39	131 ±5	158 ±12	111 ±17

Mechanical properties of the whole sinter depend on the contribution of individual phases. It should be noted that the addition of Cr_3C_2 ceramics to the surface layers during alloying leads to an increase in the hardness of layers obtained and an increase in the homogeneity of the layer obtained across its thickness. The hardness results show the improvement in strength properties after surface alloying treatment (**Figure 7**).

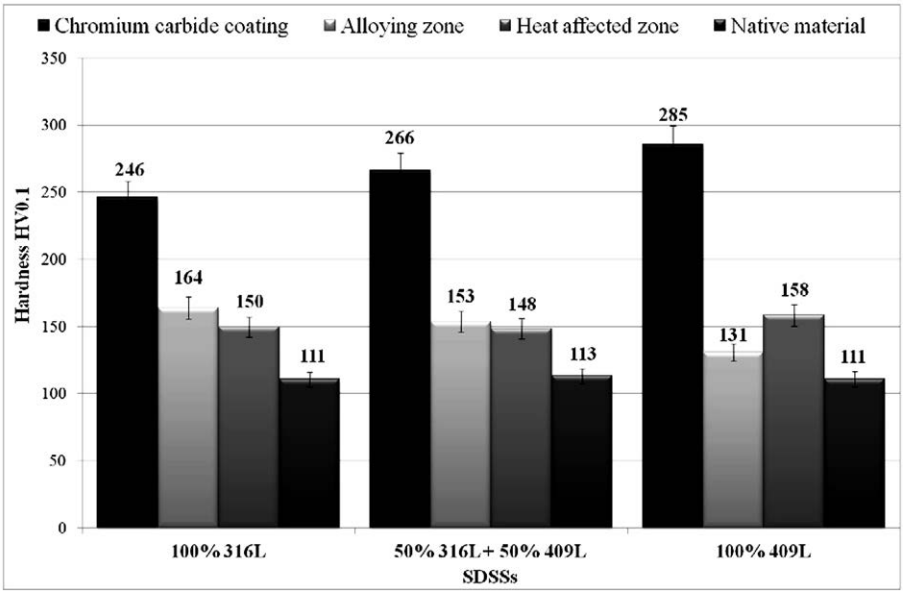

Fig. 7. Hardness of SDSSs
Rys. 7. Twardość spiekanych stali duplex

Scratch tests were performed under constant load in order to evaluate the coefficient of friction. **Table 5** presents the data of coefficient of friction for the SDSSs obtained by the scratch test.

Table 5. Coefficient of friction for the SDSSs
Tabela 5. Współczynnik tarcia dla spiekanych stali duplex

SDSSs	Coefficient of friction		
	Cr_3C_2–NiAl coating	Alloying zone	Native material
100% 316L	0.17	0.10	0.12
50% 316L + 50% 409L	0.12	0.11	0.14
100% 409L	0.14	0.12	0.15

The resistance to friction wear of SDSSs depends on several factors, such as microstructure, hardness, porosity, or surface quality. It has been shown that improved wear resistance in the group of austenitic–ferritic sinters is observed for steels with non–homogeneous microstructure and a higher level of the hardness. The modification of the coefficient of friction in the layer contributed to the improvement in tribological properties (**Figure 8**).

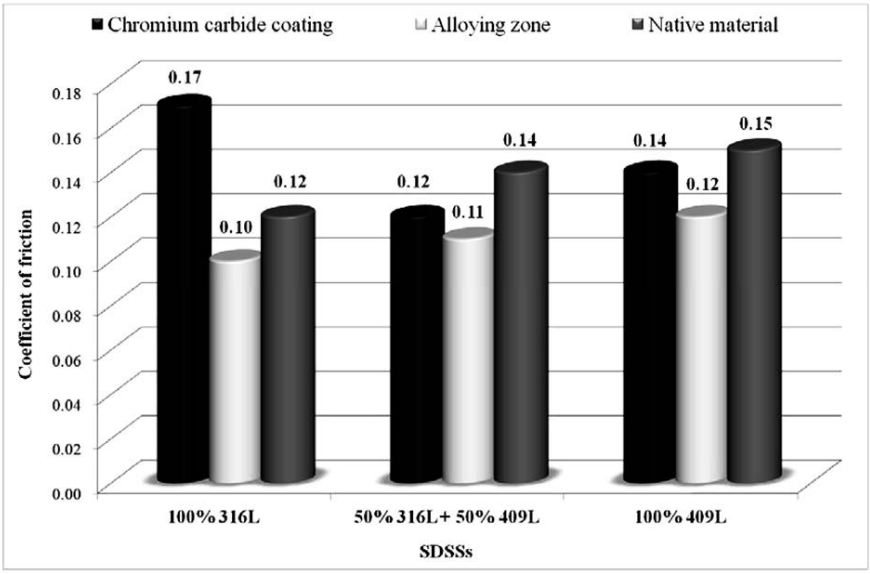

Fig. 8. Coefficient of friction for the SDSSs
Rys. 8. Współczynnik tarcia dla spiekanych stali duplex

CONCLUSIONS

The characteristic of mechanical properties of Cr_3C_2–NiAl coating and surface layers on SDSSs after alloying by the GTAW method were carried out. Taking into account excellent strength and hardness, chromium carbide (Cr_3C_2–NiAl) was applied to prepare the coating by the APS method. Furthermore, the GTAW (TIG) welding method was used to modify the surface layer of SDSSs. The results of this modification are the formation of a surface layer with a homogeneous cellular–dendritic structure.

Modification of the surface layer of SDSSs through alloying using the GTAW method led to an increase in mechanical properties and wear resistance, taking into account the coefficient of friction obtained. A valuable benefit of using this method is the opportunity for the modification of the surface in terms of hardness and the coefficient of friction. As demonstrated in the study, the GTAW method causes a decrease in the coefficient of friction and an increase in hardness, which allows for a wider use of these modern materials. Tribological properties of SDSSs depend on the chemical composition, proportion of individual powders, sintering conditions, suitable coatings, and current intensity in the applied method.

REFERENCES

1. Sheppard L.: The Powder Metallurgy Industry Worldwide 2007–2012. Materials technology Publications, 2007.
2. Peruzzo M., Beux T.D., Ordonez M.F.C., Souza R.M., Farias M.C.M.: High-temperature oxidation of sintered austenitic stainless steel containing boron or yttria. Corrosion Science, 2017, vol. 129, pp. 26–37.
3. Martín F., García C., Blanco Y., Rodriguez-Mendez M.L.: Influence of sinter-cooling rate on the mechanical properties of powder metallurgy austenitic, ferritic, and duplex stainless steels sintered in vacuum. Materials Science & Engineering A, 2015, vol. 642, pp. 360–365.
4. Asif M.M., Shrikrishna K.A., Sathiya P., Goel S.: The impact of heat input on the strength, toughness, microhardness, microstructure and corrosion aspects of friction welded duplex stainless steel joints. Journal of Manufacturing Processes, 2015, vol. 18, pp. 92–106.
5. Rajaguru J., Arunachalam N.: Coated tool Performance in Dry Turning of Super Duplex Stainless Steel. Procedia Manufacturing, 2017, vol. 10, pp. 601–611.
6. Lailatul P.H., Maleque M.A.: Surface Modification of Duplex Stainless Steel with SiC Preplacement Using TIG Torch Cladding. Procedia Engineering, 2017, vol. 184, pp. 737–742.
7. Shojaati M., Beidokhti B.: Characterization of AISI 304/AISI 409 stainless steel joints using different filler materials. Construction and Building Materials, 2017, vol. 147, pp. 608–615.
8. Paulraj P., Garg R.: Effect of welding parameters on pitting behavior of GTAW of DSS and super DSS weldments. Engineering Science and Technology, an International Journal, 2016, vol. 19, pp. 1076–1083.
9. Lisiecka B., Dudek A., Strzelczak K.: Analysis of the structure and tribological properties of sintered stainless steel. Tribologia, 2017, vol. 2, pp. 99–105
10. Espallargas N., Berget J., Guilemany J.M., Benedetti A.V.: Suegama P.H. Cr_3C_2–NiCr and WC–Ni thermal spray coatings as alternatives to hard chromium for erosion–corrosion resistance. Surface & Coatings Technology, 2008, vol. 202, pp. 1405–1417.
11. Korkmas K.: Investigation and characterization of electrospark deposited chromium carbide-based coating on the steel. Surface & Coatings Technology, 2015, vol. 272, pp. 1–7.
12. Brupbacher M.C., Zhang D., Buchta W.M., Graybeal M.L., Rhim Y.R., Nagle D.C., Spicer J.B.: Synthesis and characterization of binder-free Cr_3C_2 coatings on nickel-based alloys for molten fluoride salt corrosion resistance. Journal of Nuclear Materials, 2015, vol. 461, pp. 215–220.
13. Gariboldi E., Rovatti L., Lecis N., Mondora L., Mondora G.A.: Tribological and mechanical behaviour of Cr_3C_2–NiCr thermally sprayed coatings after prolonged aging. Surface & Coatings Technology, 2016, vol. 305, pp. 83–92.
14. Matikainen V., Bolelli G., Koivuluoto H., Sassatelli P., Lusvarghi L., Vuoristo P.: Sliding wear behaviour of HVOF and HVAF sprayed Cr_3C_2–based coatings. Wear, 2017, vol. 388–399, pp. 57–71.
15. Janka L., Berger L.M., Norpoth J., Trache R., Thiele S., Tomastik C., Matikainen V., Vuoristo P.: Improving the high temperature abrasion resistance of thermally sprayed Cr_3C_2–NiCr coatings by WC addition. Surface & Coatings Technology, 2018, vol. 337, pp. 296–305.
16. Tseng K.H., Wang N.S.: Research on bead width and penetration depth of multicomponent flux-aided arc welding of grade 316 L stainless steel. Powder Technology, 2017, vol. 311, pp. 514–521.
17. Vidyarthy R.S., Dwivedi D.K.: Activating flux tungsten inert gas welding for enhanced weld penetration. Journal of Manufacturing Processes, 2016, vol. 22, pp. 211–228.
18. Maruthi G.D., Purushotham N., Rashmi R.: Low Temperature Embrittlement studies on Stainless Steel 304 LN TIG Welds. Materials Today: Proceedings, 2018, vol. 5, pp. 2891–2900.
19. Zou Y., Ueji R., Fujii H.: Mechanical properties of advanced active-TIG welded duplex stainless steel and ferrite steel. Materials Science & Engineering A, 2015, vol. 620, pp. 140–148.